The Interaction of Angiotensin II and Milk Fat Globule Epidermal Growth Factor VIII in Proinflammatory Arterial Remodeling

Leng Ni[1,2], Lijuan Liu[1], Wanqu Zhu[1], Richard Telljohann[1], Jing Zhang[1], Robert E. Monticone[1], Kimberly R. McGraw[1], Changwei Liu[2], Christopher H. Morrell[1], Edward G. Lakatta[1], and Mingyi Wang[1]

1.Laboratory of Cardiovascular Science, National Institution on Aging, National Institutes of Health, Biomedical Research Center (BRC), 251 Bayview Boulevard, Baltimore, MD 21224, USA. 2. Department of Vascular Surgery, Peking Union Medical College Hospital, Peking Union Medical College & Chinese Academy of Medical Sciences, China.

Running title: Arterial Proinflammatory Remodeling

Correspondence to Mingyi Wang, MD, PhD, FAHA

Laboratory of Cardiovascular Science

National Institution on Aging

National Institutes of Health

Biomedical Research Center (BRC)

251 Bayview Boulevard, Baltimore, MD 21224, USA

Email: mingyiw@grc.nia.nih.gov

Tel: (+1) 410-558-8112

Abstract

Angiotensin II (Ang II) and milk fat globule-epidermal growth factor VIII (MFG-E8) are increased in the aged arterial wall and are involved in remodeling. However, the precise interactions between Ang II and MFG-E8 in proinflammatory arterial remodeling remains unknown. In this study, both MFG-E8 knock out (KO) and wild-type (WT) mice were infused with Ang II via an osmotic mini-pump. After infusion with Ang II, increases in systolic blood pressure (SBP) and circulating Ang II were observed in all animals, but changes to the aortic molecular, cellular, and structural remodeling were dependent on genotype (presence or absence of MFG-E8) ($p<0.05$, two-way ANOVA): (1) Ang II infusion substantially increased intimal-medial thickness, elastic lamina degradation, collagen deposition, and proliferation of vascular smooth muscle cells (VSMCs) in the aortic walls in WT; in contrast, in MFG-E8 KO mice, these cellular and matrix effects were significantly reduced; (2) Ang II treatment significant increased the activation and expression of matrix metallopeptidase type 2 (MMP-2), activated transforming growth factor-beta 1 (TGF-β1) and its downstream signaling molecule phosphorylation mothers against decapentaplegic homolog 2 (p-Smad2), and collagen type I production in the aortic walls of WT mice, however, in KO mice, these molecular effects were significantly reduced; (3) Ang II treatment increased nuclear factor-kappa beta (NF-κB) p65, monocyte chemoattractant protein-1 (MCP-1), and tumor necrosis factor-alpha 1 (TNF-α) protein expression by at least two fold in the aortic walls of WT mice, conversely, in MFG-E8 KO mice, no significant proinflammatory changes were found. Taken together, these findings suggest that Ang II effects on proinflammatory arterial remodeling are MFG-E8 genotype - dependent.

Key Words: Aging ● Angiotensin II ● Milk fat globule-epidermal growth factor 8 ● Proinflammation ● Arterial remodeling

Introduction

Angiotensin II (Ang II), a major metabolic component of the renin-angiotensin-aldosterone signaling system, produces multiple cardiovascular effects[1, 2]. Physiologically, Ang II signaling is critical in regulating blood pressure. In pathological conditions, Ang II stressor signaling induces proinflammation, contributing to the development of hypertensive vasculopathy[1, 3]. Our previous study showed that young adult animals infused with Ang II exhibited "older" arterial phenotypes, including intimal vascular smooth muscle cells (VSMC) infiltration, intimal-medial thickening (IMT), matrix metalloproteinase type 2 activation (MMP-2), transforming growth factor beta (TGF-β1) activation, collagen deposition, eventually leading to elevated systolic blood pressure (SBP)[4].

Milk fat globule-epidermal growth factor 8 (MFG-E8) is a secreted glycoprotein enriched in the milk fat globule that was initially discovered as a bridging molecule between apoptotic cells and macrophages for the clearance of cellular debris, known as efferocytosis [5, 6]. It is also known to be involved in inflammatory vascular conditions[7-13]. Prior *in vivo* studies have demonstrated that the MFG-E8 protein increases during arterial aging and arterial injury, and in hypertensive, diabetic, and atherosclerotic arterial walls [7-12, 14]. Additionally, MFG-E8 is a pivotal relay element within the Ang II/monocyte chemoattractant protein-1 (MCP1) signaling cascade that mediates VSMC proinflammation, invasion and proliferation[7, 8] . These *in vivo* and *in vitro* studies indicate that VSMC cellular and molecular events play a potential causal role in the initiation and progression of Ang II associated adverse arterial inflammatory remodeling such as IMT.

Ang II and MFG-E8 are simultaneously increased in the proinflamed aging arterial wall or cultured aging VSMCs[7, 8], however, their precise interactions during remodeling remain unknown. Therefore, we studied, young adult (30-week-old) MFG-E8 knock out (KO) and aged match wild-type (WT) mice which were infused with Ang II via an osmotic mini-pump to investigate how Ang II interacts with MFG-E8 in the proinflamed arterial wall at the molecular, cellular, and tissue levels.

Materials and Methods

All data, analytic methods, and study materials will be made available to other researchers for purposes of reproducing the results or replicating the procedure. The material that supports the findings of this study are available from the corresponding author upon reasonable request.

Experimental Animals

All experiments were conducted according to the protocols (445-LCS-2022) approved by the National Institute on Aging (NIA) in accordance with the National Institute of Health (NIH) Animal Care and Use Committee. MFG-E8 knock out (KO) mice were obtained from Dr. Mark Udey in National Cancer Institute (NCI), and generated, characterized, and genotyped as described previously.[15, 16] Transgenic Rip1-Tag2 mice were obtained from the National Cancer Institute (NCI). MFG-E8 KO mice were generated by replacing exons 2 to 6 of the gene encoding MFG-E8 in 129SvJ ES cells with a neomycin resistance cassette. Mice were genotyped by PCR using the following primers: Rip1-Tag2, GGACAAACCACAACTAGAATGCAGTG (forward) and CAGAGCAGAATTGTGGAGTGG (reverse); Neo, GCCAGAGGCCACTTGTGTAG; and MFG-E8, CTCTCAGATTCACCTGCTCGTG and CACCGTTCAGGCACAGGCTG. 30-week-old male MFGE8 KO mice (homozygous for lack of MFG-E8) and age-matched wide-type (WT) mice were used in this study.

Angiotensin II Infusion and Blood Pressure Measurement

Osmotic mini-pumps (Alzet Model 2004) were implanted dorsally and subcutaneously in anaesthetized (2% isoflurane) mice (n=12/group) to deliver Ang II (500 ng/kg/min) or 0.9% saline (placebo) for 28 days.

Systolic blood pressure (SBP) was measured using the pneumatic tail-cuff method (MRBP System, Life Science, Woodland Hills, California). Briefly, animals were placed in a plastic chamber maintained at 34°C and a cuff with a pneumatic pulse sensor were attached to the tail for SBP measurements. Mice were trained for one week to become accustomed to the new handling and environment. Once SBP values were consistent, eight consecutive measurements were performed for each mouse and all the values collected were averaged. Blood pressure was monitored 1 week prior to mini-pump implantation (baseline), and once per week from day 7 to 28 after the pump implantation.

Sample Collection and Preparation

Blood Collection

Ocular blood was collected at 14 days post mini pump implantation. In the last week of the experiment, mice were sacrificed under sodium pentobarbital anesthesia, and blood was collected from the right atrium into a 4ml Ethylenediaminetetraacetic acid (EDTA) coated Eppendorf tubes immediately. The blood samples were centrifuged for 15 minutes at 3000 rpm (1500 × g) at 4°C. The supernatant was carefully transferred into 0.5 ml Eppendorf tube and stored at -80°C.

Tissue Collection

Tissue samples were isolated from the ascending aorta to the bifurcation of the common iliac artery. For morphological analysis, animals were perfused with 4% paraformaldehyde-Phosphate buffered saline (PBS) at physiological pressure for 5 minutes; and abdominal aortic tissues were paraffin-embedded and sectioned for histology study. For western blotting, animals were perfused with 0.9% saline, fresh aortic tissues were snap-frozen in liquid nitrogen and stored at –80°C refrigerator until use.

Histology, Immunostaining, and Morphometric analyses

To quantitate aortic remodeling, intimal to media thickness was measured using hematoxylin and eosin (H&E) staining; elastin breaks were counted via Elastin Verhoeff's-Van Gieson (EVG) staining; and collagen deposition was evaluated with Masson's trichrome staining. H&E, EVG, and Masson trichrome staining were performed using MasterTech stain kits (StatLab, McKinney, TX). Staining of aortic walls were performed as described in previous studies [17]. In brief, aortic paraffin sections (5 µm in thickness) were utilized for immunostaining with anti-in-intercellular adhesion molecule 1 (ICAM1), vascular cell adhesion molecule 1 (VCAM1), and collagen type I antibodies. Details of primary antibodies used are listed in **Table 1**. The ratios of target immunohistochemical staining positive area to the total tissue or cell area were determined via computer-imaging program according to the instruction provided by manufacture (MetaMorph Imaging System, Molecular Devices, San Jose, CA).

Western Blotting

Western blot analysis was performed as described previously[17]. In brief, total protein was quantified using the Pierce™ Coomassie (Bradford) protein assay kit (Hercules, CA, USA), following the manufacturer's instructions. 10 µg of total protein was run on 4-12%

NuPAGE gels (Thermo Fisher Scientific, Waltham, MA), transferred to a polyvinylidene fluoride (PVDF) membrane, and immunoblotted with antibodies listed in **Table 1.** Western blotting bands were quantified using NIH image J (http://rsb.info.*nih*.gov/*nih-image*/) and the intensity values were normalized to loading control GAPDH.

PAGE Zymography

MMP-2 activity was determined via Polyacrylamide Gel Electrophoresis (PAGE) gelatin zymography (Thermo Fisher Scientific, Waltham, MA) as described previously[18].

Ang II Quantification

RayBio® Mouse MFG-E8 ELISA Kit, a commercially available enzyme-linked immunosorbent assay (ELISA) kit, (RayBiotech Life, Peachtree Corners, GA) was used to measure the amount of Ang II in mouse plasma.

Statistical analysis

All experiments were performed with at the least four animals/group. All data were presented as mean ± SEM. Statistical analyses used two-way or two-way repeated measure ANOVA followed by Bonferroni post hoc test used for multiple comparisons. These statistical analyses were performed using GraphPad Prism (version 7.0) software. For SBP, the repeated-measures data are analyzed using a linear mixed-effects model [19]. A value of $p \leq 0.05$ was considered statistically significant.

Results

Ang II infusion increases circulating Ang II, aortic MFG-E8, and systolic blood pressure

Vasoactive mediator Ang II and blood pressure play a causal role in proinflammatory arterial remodeling[1, 20]. Ang II infusion markedly increased the levels of circulating Ang II in both WT and KO mice on day 14 and day 28 (two-way repeated ANOVA analysis of treatment x genotype indicated no interaction: $p>0.05$), compared to saline infused animals (**Figure 1A**). Importantly, Ang II infusion dramatically increased the abundance of aortic MFG-E8 in WT as compared to saline control mice. We confirmed that aortic MFG-E8 protein, however, was not detected in the KO mice infused with either Ang II or saline (**Figure 1B & C**).

The repeated two-way ANOVA analysis showed that SBP had a statistically significant interaction ($p = 1.464e-12$) of treatment x genotype (**Figure 1D).** At baseline (time=day 0) there was no difference in SBP between any of the groups. However, after infusing the animals with Ang II for 28 days, both WT and KO, showed significantly increased SBP levels compared to saline infused animals. Unexpectedly, in KO the SBP of Ang II infused mice, were significantly elevated ($p<0.05$) when compared to WT. Thus, these finding suggest that KO mice are more sensitive than WT to Ang II infusion and leads to an increased SBP. Overall, after infusing with Ang II we observed increases in SBP and circulating Ang II were observed in all animals, independent of genotype.

Ang II infusion reduces activation of aortic MMP-2 in KO mice.

Increases in circulating Ang II and blood pressure enhance the activity of MMP-2[4]. Gelatinase MMP-2 activation plays a crucial role in the process of adverse arterial remodeling such as IMT and SBP increase [20]. To determine whether the interactive effects of treatment and genotype on the expression and activity of gelatinases MMP-2, PAGE zymography and Western blotting analysis were performed. Zymography demonstrated that the levels of activated MMP-2 within the aortic walls in mice after Ang II infusion were dependent upon genotype ($p<0.01$, by two-way ANOVA) (**Figure 2A)**. In WT mice, Ang II infusion markedly increased the levels of activated aortic MMP-2 compared to saline. In KO animals, activated MMP-2 in Ang II infused animals was significantly higher than saline, but was significantly less than that of the WT Ang II treated animals (**Figure 2A)**. Western blotting analysis showed that the abundance of aortic MMP-2 protein induced by Ang II was dependent upon genotype (**Figure 2B).** In WT mice, Ang II markedly increased the levels of MMP-2 protein in aortic walls when compared to saline **(Figure 2B)**. In KO mice, the MMP-2 protein levels were significantly increased in Ang II versus saline animals but was significantly less than that of the WT Ang II treated animals **(Figure 2B)**. Similarly, the abundance of MT1MMP, an activator of MMP-2, induced by Ang II, was increased dependent upon genotypes ($p<0.01$, followed by two-way ANOVA) (**Figure 2B)**. In WT mice, Ang II significantly increased the levels of MT1MMP protein in the aortic wall compared to saline ($p<0.001$). However, in KO animals, MT1MMP protein levels showed no significant increase ($p>0.05$) (**Figure 2B)**.

The above findings demonstrate that Ang II and MFG-E8 are both needed for the increased activation and expression of MMP-2 in the aortic walls of mice,

Ang II infusion does not increase aortic TGF- β1 fibrotic signaling in KO mice.

Ang II signaling and its subsequent blood pressure elevation, as well as MMP-2 activation, all promote TGF-β1 activation and its fibrotic effect within arterial walls *in vivo* and in cultured VSMCs[4, 20, 21]. Western blotting analysis demonstrated that the Ang II-induction of activated arterial TGF-β1 was dependent upon genotype ($p<0.001$, by two-way ANOVA) (**Figure 3A & 3B)**. In WT mice, Ang II infusion markedly increased the levels of activated TGF-β1 protein in the aortic walls, while in KO mice there was a smaller significant increase when compared to saline (**Figure 3A & 3B)**. Notably, in Ang II infused animals, the levels of TGF-β1 protein in the WT was significantly higher than those found in KO (**Figure 3A & 3B)**. Similarly, Western blotting analysis demonstrated that the Ang II induction of arterial TGF-β1 downstream signaling molecule increased SMAD2 phosphorylation (p-SMAD2) and was also dependent upon genotype ($p<0.001$, by two-way ANOVA) (**Figure 3A & 3B).** In WT mice, Ang II infusion markedly increased the levels of activated p-SMAD2 protein in the aortic walls compared to saline; in contrast, in KO mice there was no significant increase of these proteins with Ang II (**Figure 3A & 3B)**. Expectedly, immunohistostaining and Western blotting analyses indicated that the Ang II induction of arterial TGF-β1/p-SMAD2 downstream signaling product, collagen I levels, were dependent upon genotype ($p<0.001$, by two-way ANOVA) (**Figure 3C).** In WT mice, Ang II infusion markedly increased the levels of collagen type I protein in the aortic walls compared to saline infusion; in contrast, in KO mice there was no significant increase of this protein when treated with Ang II **(Figure 3C)**.

We observed that both Ang II and MFG-E8 are both needed to for the increased activation of TGF-β1 and its downstream signaling molecule, p-Smad2, in the aortic walls of mice.

Ang II infusion activates NF-κB signaling in both WT and KO mice and reduces its downstream proinflammatory effectors in KO mice.

NF-κB is a prominent proinflammatory transcription factor in inflamed arterial walls[22, 23]. NF-κB p65, an element of NF-κB activation, facilitates its downstream inflammatory effectors MCP1, TNF-α, ICAM1, and VCAM1 upregulation, which are typically involved in the process of arterial inflammation[23-25].

Western blotting analyses showed that the abundance of arterial NF-κB protein p65 in mice infused with Ang II was dependent on genotype ($p<0.05$, by two-way ANOVA) (**Figure 4A**). NF-κB p65 protein abundance was markedly upregulated in WT mice infused with Ang II versus saline, whereas the protein levels remained at a similar level in both groups of KO animals (**Figure 4A)**. In the saline infused mice, there was a significant increase in NF-κB levels when WT and KO are compared. Western blotting indicated that the abundance of aortic MCP1 protein induced by Ang II in mice was also dependent upon genotype (**Figure 4A,** $p<0.0001$ by two-way ANOVA**).** WT mice infused with Ang II showed significant increases in the levels of activated MCP1 protein in the aortic wall compared to saline; conversely, KO mice infused with Ang II slightly increased MCP1 protein expression but did not reach significant levels when compared to saline (**Figure 4A).** Notably, when mice were treated with Ang II, MCP1 protein levels were lower in KO versus WT (**Figure 4A**). Western blotting and immunostaining analyses also revealed that Ang II infusion altered TNF-α protein levels in mice and was dependent upon genotype (**Figure 4A & B,** $p<0,0001$ by two-way ANOVA). The levels of TNF-α protein in WT mice increased approximately three-fold in the aortic wall when infused with Ang II compared to saline, however, the protein levels in KO mice were not significantly altered in either treatment

group (**Figure 4A & B).** In addition**,** immunohistostaining and morphometric analysis demonstrated that the increased levels of arterial adhesive molecules ICAM1 and VCAM1 protein in mice induced by Ang II were also dependent upon genotype **(Figure 4C)**, both $p<0.0001$ by two-way ANOVA**).** In WT mice Ang II infusion markedly increased the protein levels of both ICAM1 and VCAM1 in the aortic wall compared to saline (both $p<0.0001$), however, in KO mice Ang II infusion did not significantly alter either ICAM1 or VCAM1protein abundance versus saline (**Figure 4D).**

These findings show that Ang II and MFG-E8 both need to be present to increase MCP-1 and TNF-α, and VCAM1 protein expression in the aortic walls of mice,

Ang II infusion induced arterial cellular and matrix remodeling is reduced in KO mice.

Immunohistochemistry of mice aortic walls was performed after Ang II or saline infusion. The morphometrical analysis indicated that adverse arterial remodeling was dependent upon genotype, which may be related to proinflammatory molecular remodeling and changes in SBP (**Figure 1-4**). In WT mice a marked increase in IMT was observed in the aortic walls in mice infused with Ang II compared to saline, however in KO mice, the significant difference in IMT was not observed (**Figure 5A)**. In WT mice treated with Ang II, EVG staining indicated a significant increase in the number of the elastin fiber breaks versus saline, while this effect was substantially reduced in KO mice (**Figure 5B**). In WT mice infused with Ang II, Masson's trichrome staining showed that the fraction of extracellular matrix (ECM), mainly collagen, was increased versus saline, while this effect was not observed in KO mice (**Figure 5C**). The proliferation of VSMCs is a key cellular event of arterial thickening in hypertension induced by Ang II[26]. In WT mice infused with Ang II, the percentage of proliferating cell nuclear antigen

(PCNA) positive VSMCs, an index of cellular division, was markedly elevated when compared to saline, however, no difference in PCNA was seen in KO animals (**Figure 5D)**. Notable, in Ang II infused animals, the amount of PCNA in WT mice was significantly elevated when compared to KO (**Figure 5D)**.

The above results indicate that when both Ang II and MFG-E8 are present there is a substantial increase in IMT, elastic lamina degradation, collagen deposition, and proliferation of VSMCs in the aortic walls of mice.

Discussion

MFG-E8 plays an important role in arterial wall remodeling. We demonstrated that Ang II synergistically interacts with MFG-E8 during arterial inflammatory remodeling *in vivo* under experimental hypertensive conditions (**Figure 6**). The absence of MFG-E8 alleviates Ang II induced proinflammatory remodeling at the molecular, cellular, and tissue levels, independent of SBP levels, in experimentally induced hypertensive mice. However, the presence of MFG-E8 prevents arterial wall inflammation and thickening under unstressed normotensive conditions.

Ang II infusion elevates circulating Ang II levels and induces SBP increases, leading to the development of hypertension in mice, independent of MFG-E8 expression. Ang II increases MFG-E8 in the aortae of mice. Aortic MFG-E8 is increased in renal hypertensive rats[27]. Increased Ang II is colocalized with elevated MFG-E8 within old human aortic walls[8]. These findings seem to provide evidence that MFG-E8 mediates Ang II associated increases in SBP. Intriguingly, our findings also demonstrate that Ang II infusion increases circulating Ang II and raises the SBP in both KO and WT mice, revealing that the Ang II downstream molecule MFG-E8 may have a small effect on SBP increase in these animals.

Ang II infusion induces aortic MMP-2 and TGF-ß1 activation, promoting arterial elastic degeneration and fibrosis, dependent on the interaction of MFG-E8 and Ang II expression under hypertensive conditions (**Figures 2 & 3)**. Ang II-induced arterial MMP-2 activation is markedly increased in WT rather than KO mice, which is related to an increase of MT1MMP, an activator of MMP-2. We observed that treating VSMCs with recombinant human MFG-E8 (rhMFG-E8) increases the activation of MMP-2 [28, 29]. These findings support a concept that MFG-E8 is a

potent inducer of MMP-2 activation. Notably, activated MMP-2 has a high capacity to degrade aortic elastin laminae and subsequently releases activated TGF-ß1 [4, 20, 21, 29, 30]. Ang II infusion induces greater arterial TGF-ß1 activation in the aortic walls of WT rather than KO mice suggesting that the synergy of Ang II with MFG-E8 signaling is involved in TGF-ß1 activation, which may be associated with MMP-2 activation. MMP-2, a potent activator of latent TGF binding protein (LTBP), facilitates the conversion from the latent to the active form[21]. We also have observed that treating VSMCs with rhMFG-E8 increase the fibrogenic TGF-ß1/SMAD2/collagen type I signaling cascade [28]. Thus, TGF-β1 fibrogenic signaling plays a causal role in adverse arterial remodeling [21, 31].

Ang II infusion increases NF-κB pathway which elevates proinflammation associated with activation of NF-κB, dependent upon MFG-E8 expression, in the arterial wall and is dependent on the interaction of MFG-E8 and Ang II (**Figure 4**). NF-κB p65 is a core element of NF-κB activation during proinflammatory arterial wall remodeling[32]. When WT mice were infused with Ang II, NF-κB was [32] markedly increased in WT but not in KO, suggesting that MFG-E8 is an important intermediary of NF-κB signaling. Several studies indicate that NF-κB activation facilitates the production of MCP1, TNF-α, ICAM1, and VCAM1 during the processes of arterial inflammation and remodeling[14, 23-25, 33-37]. The upregulation of MCP1 and TNF-α is higher in WT mice than in KO suggesting MFG-E8 involvement. MFG-E8 increases MCP1 activation in VSMCs[8]. MCP1 and TNF-α are prominent inflammatory factors in arterial walls[38]. Ang II also induced the levels of arterial ICAM1 and VCAM1 upregulation and is dependent on the interaction of MFG-E8 and Ang II. Ang II increases NF-κB and its downstream molecules MCP1, TNF-α, ICAM1 and VCAM1 via MFG-E8 signaling, facilitating arterial inflammation in mice under pressure which drives remodeling.

Ang II infusion of mice promotes adverse arterial remodeling, including IMT, collagen deposition, elastic fiber degradation, proliferation of VSMCs, dependent upon the presence or absence of MFG-E8 (**Figure 5**). MFG-E8 deficiency substantially alleviates Ang II induced adverse arterial remodeling including IMT, collagen deposition and elastic fiber breakdown in KO vs WT, which have hypertension. Increases in arterial MMP-2 activation, TGF-β fibrotic signaling, inflammation, proliferation of VSMCs in mice are the molecular and cellular mechanisms of arterial elastic network collapse, collagen deposition, and IMT[2, 7-10, 12, 13, 18, 20, 29, 38].

Notably, our current findings indicate that KO mice with the absence of MFG-E8 exhibited increased SBP, or hypertension, and that they still had reduced Ang II induced inflammation and tissue remodeling. Unexpectedly, the levels of NF-kB p65 and IMT were significantly increased in the aortic walls of KO versus WT animals treated with saline, which we regarded as "physiologic normotensive conditions" (**Figure 4 & 5)**. These confounding results may demonstrate a weakness in our model and further studies should be conducted. It is known that MFG-E8 is a bridging molecule for the clearance of apoptotic cellular debris and exhibits an anti-inflammatory role under certain conditions[39-41]. Thus, low levels of MFG-E8 may play a possible anti-inflammatory role. Further studies are needed to investigate the anti-inflammatory role of MFG-E8 in the arterial wall in physiologic conditions.

Perspectives

Both Ang II and MFG-E8 are involved in proinflammatory arterial remodeling. MFG-E8 is a downstream molecule of Ang II signaling in VSMCs *in vitro* and in the arterial wall *in vivo*. Ang II interacts with MFG-E8 at the molecular, cellular and tissue levels under pressure. MFG-E8

signaling is a key molecular event for Ang II induced adverse arterial remodeling via the increase of proinflammation, VSMC proliferation, collagen deposition, and elastin fragmentation. These findings suggest that MFG-E8 collaborates with Ang II to increase proinflammation in adverse arterial wall remodeling. Thus, targeting the MFG-E8/Ang II synergy could be a novel approach to maintaining the health of the arterial system.

Conflicts of Interest

None

Sources of Funding

This research was supported by the Intramural Research Program of the National Institute on Aging, National Institutes of Health, the National Natural Science Foundation of China (No.81470585) and the Fundamental Research Funds for the Central Universities (No. 3332019028).

Disclosures

None.

References

1. Ferrario CM, Strawn WB. Role of the renin-angiotensin-aldosterone system and proinflammatory mediators in cardiovascular disease. *Am J Cardiol*. 2006;98:121-128
2. Wang M, Jiang L, Monticone RE, Lakatta EG. Proinflammation: The key to arterial aging. *Trends in endocrinology and metabolism: TEM*. 2014;25:72-79
3. Gromotowicz-Poplawska A, Szoka P, Kolodziejczyk P, Kramkowski K, Wojewodzka-Zelezniakowicz M, Chabielska E. New agents modulating the renin-angiotensin-aldosterone system-will there be a new therapeutic option? *Exp Biol Med (Maywood)*. 2016;241:1888-1899
4. Wang M, Zhang J, Spinetti G, Jiang LQ, Monticone R, Zhao D, Cheng L, Krawczyk M, Talan M, Pintus G, Lakatta EG. Angiotensin ii activates matrix metalloproteinase type ii and mimics age-associated carotid arterial remodeling in young rats. *The American journal of pathology*. 2005;167:1429-1442
5. Borisenko GG, Iverson SL, Ahlberg S, Kagan VE, Fadeel B. Milk fat globule epidermal growth factor 8 (mfg-e8) binds to oxidized phosphatidylserine: Implications for macrophage clearance of apoptotic cells. *Cell Death Differ*. 2004;11:943-945
6. Atabai K, Fernandez R, Huang X, Ueki I, Kline A, Li Y, Sadatmansoori S, Smith-Steinhart C, Zhu W, Pytela R, Werb Z, Sheppard D. Mfge8 is critical for mammary gland remodeling during involution. *Mol Biol Cell*. 2005;16:5528-5537
7. Wang M, Fu Z, Wu J, Zhang J, Jiang L, Khazan B, Telljohann R, Zhao M, Krug AW, Pikilidou M, Monticone RE, Wersto R, Van Eyk J, Lakatta EG. Mfg-e8 activates proliferation of vascular smooth muscle cells via integrin signaling. *Aging cell*. 2012;11:500-508
8. Fu Z, Wang M, Gucek M, Zhang J, Wu J, Jiang L, Monticone RE, Khazan B, Telljohann R, Mattison J, Sheng S, Cole RN, Spinetti G, Pintus G, Liu L, Kolodgie FD, Virmani R, Spurgeon H, Ingram DK, Everett AD, Lakatta EG, Van Eyk JE. Milk fat globule protein epidermal growth factor-8: A pivotal relay element within the angiotensin ii and monocyte chemoattractant protein-1 signaling cascade mediating vascular smooth muscle cells invasion. *Circ Res*. 2009;104:1337-1346
9. Soubeyrand S, Nikpay M, Turner A, Dang AT, Herfkens M, Lau P, McPherson R. Regulation of mfge8 by the intergenic coronary artery disease locus on 15q26.1. *Atherosclerosis*. 2019;284:11-17
10. Viola JR, Lemnitzer P, Paulin N, Drechsler M, Nazari-Jahantigh M, Maas S, De Jong RJ, Winter J, Schober A, Weber C, Atabai K, Soehnlein O. Deletion of mfge8 inhibits neointima formation upon arterial damage. *Thromb Haemost*. 2018;118:1340-1342
11. Wang M, Wang HH, Lakatta EG. Milk fat globule epidermal growth factor viii signaling in arterial wall remodeling. *Curr Vasc Pharmacol*. 2013;11:768-776
12. Chiang HY, Chu PH, Lee TH. Mfg-e8 mediates arterial aging by promoting the proinflammatory phenotype of vascular smooth muscle cells. *J Biomed Sci*. 2019;26:61
13. Ni YQ, Zhan JK, Liu YS. Roles and mechanisms of mfg-e8 in vascular aging-related diseases. *Ageing Res Rev*. 2020;64:101176
14. Zhao H, Zhang H, Qin X. Agerelated differences in serum mfge8, tgfbeta1 and correlation to the severity of atherosclerosis determined by ultrasound. *Mol Med Rep*. 2017;16:9741-9748
15. Motegi S, Leitner WW, Lu M, Tada Y, Sardy M, Wu C, Chavakis T, Udey MC. Pericyte-derived mfg-e8 regulates pathologic angiogenesis. *Arterioscler Thromb Vasc Biol*. 2011;31:2024-2034

16. Neutzner M, Lopez T, Feng X, Bergmann-Leitner ES, Leitner WW, Udey MC. Mfg-e8/lactadherin promotes tumor growth in an angiogenesis-dependent transgenic mouse model of multistage carcinogenesis. *Cancer Res*. 2007;67:6777-6785
17. Wang M, Takagi G, Asai K, Resuello RG, Natividad FF, Vatner DE, Vatner SF, Lakatta EG. Aging increases aortic mmp-2 activity and angiotensin ii in nonhuman primates. *Hypertension*. 2003;41:1308-1316
18. Jiang L, Wang M, Zhang J, Monticone RE, Telljohann R, Spinetti G, Pintus G, Lakatta EG. Increased aortic calpain-1 activity mediates age-associated angiotensin ii signaling of vascular smooth muscle cells. *PloS one*. 2008;3:e2231
19. Verbeke G, Molenberghs G. *A linear mixed models for longitudinal data*. New York: Springer; 2009.
20. Wang M, Zhang J, Telljohann R, Jiang L, Wu J, Monticone RE, Kapoor K, Talan M, Lakatta EG. Chronic matrix metalloproteinase inhibition retards age-associated arterial proinflammation and increase in blood pressure. *Hypertension*. 2012;60:459-466
21. Wang M, Zhao D, Spinetti G, Zhang J, Jiang LQ, Pintus G, Monticone R, Lakatta EG. Matrix metalloproteinase 2 activation of transforming growth factor-beta1 (tgf-beta1) and tgf-beta1-type ii receptor signaling within the aged arterial wall. *Arterioscler Thromb Vasc Biol*. 2006;26:1503-1509
22. Wang M, Shah AM. Age-associated pro-inflammatory remodeling and functional phenotype in the heart and large arteries. *Journal of molecular and cellular cardiology*. 2015;83:101-111
23. Wortmann M, Skorubskaya E, Peters AS, Hakimi M, Bockler D, Dihlmann S. Necrotic cell debris induces a nf-kappab-driven inflammasome response in vascular smooth muscle cells derived from abdominal aortic aneurysms (aaa-smc). *Biochem Biophys Res Commun*. 2019;511:343-349
24. Jia Z, Nallasamy P, Liu D, Shah H, Li JZ, Chitrakar R, Si H, McCormick J, Zhu H, Zhen W, Li Y. Luteolin protects against vascular inflammation in mice and tnf-alpha-induced monocyte adhesion to endothelial cells via suppressing ikappabalpha/nf-kappab signaling pathway. *J Nutr Biochem*. 2015;26:293-302
25. Milstone DS, Ilyama M, Chen M, O'Donnell P, Davis VM, Plutzky J, Brown JD, Haldar SM, Siu A, Lau AC, Zhu SN, Basheer MF, Collins T, Jongstra-Bilen J, Cybulsky MI. Differential role of an nf-kappab transcriptional response element in endothelial versus intimal cell vcam-1 expression. *Circ Res*. 2015;117:166-177
26. Ozasa Y, Akazawa H, Qin Y, Tateno K, Ito K, Kudo-Sakamoto Y, Yano M, Yabumoto C, Naito AT, Oka T, Lee JK, Minamino T, Nagai T, Kobayashi Y, Komuro I. Notch activation mediates angiotensin ii-induced vascular remodeling by promoting the proliferation and migration of vascular smooth muscle cells. *Hypertens Res*. 2013;36:859-865
27. Lin YP, Hsu ME, Chiou YY, Hsu HY, Tsai HC, Peng YJ, Lu CY, Pan CY, Yu WC, Chen CH, Chi CW, Lin CH. Comparative proteomic analysis of rat aorta in a subtotal nephrectomy model. *Proteomics*. 2010;10:2429-2443
28. Wang M, Fu Z, Lakatta EG, Van Eyk J. Method for the diagnosis of age-associated vascular disorders. 2012
29. Kim SH, Liu L, Ni L, Zhang L, Zhang J, Wang Y, . McGraw KR, Monticone R, Telljohann R, Lakatta EG. Mfg-e8 signaling promotes elastolysis and calcification in the aging aortic wall. *biorxiv*. 2020:https://doi.org/10.1101/2020.1110.1105.32672
30. Wang M, Kim SH, Monticone RE, Lakatta EG. Matrix metalloproteinases promote arterial remodeling in aging, hypertension, and atherosclerosis. *Hypertension*. 2015;65:698-703
31. Harvey A, Montezano AC, Lopes RA, Rios F, Touyz RM. Vascular fibrosis in aging and hypertension: Molecular mechanisms and clinical implications. *Can J Cardiol*. 2016;32:659-668

32. Monaco C, Paleolog E. Nuclear factor kappab: A potential therapeutic target in atherosclerosis and thrombosis. *Cardiovasc Res*. 2004;61:671-682
33. Ogbozor UD, Opene M, Renteria LS, McBride S, Ibe BO. Mechanism by which nuclear factor-kappa beta (nf-kb) regulates ovine fetal pulmonary vascular smooth muscle cell proliferation. *Mol Genet Metab Rep*. 2015;4:11-18
34. Yu F, Li BY, Li XL, Cai Q, Zhang Z, Cheng M, Yin M, Wang JF, Zhang JH, Lu WD, Zhou RH, Gao HQ. Proteomic analysis of aorta and protective effects of grape seed procyanidin b2 in db/db mice reveal a critical role of milk fat globule epidermal growth factor-8 in diabetic arterial damage. *PloS one*. 2012;7:e52541
35. Cheng M, Li BY, Li XL, Wang Q, Zhang JH, Jing XJ, Gao HQ. Correlation between serum lactadherin and pulse wave velocity and cardiovascular risk factors in elderly patients with type 2 diabetes mellitus. *Diabetes Res Clin Pract*. 2012;95:125-131
36. Li Y, Ran W, Zhang J, Chen S, Li Y, Luo D, Wang C, Jia W. Circulating milk fat globule-epidermal growth factor 8 levels are increased in pregnancy and gestational diabetes mellitus. *J Diabetes Investig*. 2017;8:571-581
37. Li Y, Ran W, Zhang J, Chen S, Li Y, Luo D, Wang C, Jia W. Elevated serum milk fat globule-epidermal growth factor 8 levels in type 2 diabetic patients are suppressed by overweight or obese status. *IUBMB Life*. 2017;69:63-71
38. Spinetti G, Wang M, Monticone R, Zhang J, Zhao D, Lakatta EG. Rat aortic mcp-1 and its receptor ccr2 increase with age and alter vascular smooth muscle cell function. *Arterioscler Thromb Vasc Biol*. 2004;24:1397-1402
39. Li BZ, Zhang HY, Pan HF, Ye DQ. Identification of mfg-e8 as a novel therapeutic target for diseases. *Expert Opin Ther Targets*. 2013;17:1275-1285
40. Ait-Oufella H, Kinugawa K, Zoll J, Simon T, Boddaert J, Heeneman S, Blanc-Brude O, Barateau V, Potteaux S, Merval R, Esposito B, Teissier E, Daemen MJ, Leseche G, Boulanger C, Tedgui A, Mallat Z. Lactadherin deficiency leads to apoptotic cell accumulation and accelerated atherosclerosis in mice. *Circulation*. 2007;115:2168-2177
41. Atabai K, Jame S, Azhar N, Kuo A, Lam M, McKleroy W, Dehart G, Rahman S, Xia DD, Melton AC, Wolters P, Emson CL, Turner SM, Werb Z, Sheppard D. Mfge8 diminishes the severity of tissue fibrosis in mice by binding and targeting collagen for uptake by macrophages. *J Clin Invest*. 2009;119:3713-3722

Novelty and Significance

What Is Known?

- Both Ang II and MFG-E8 increase with age and are involved in proinflammatory arterial remodeling.

What New Information Does This Article Contribute?

- Ang II interacts with MFG-E8 at the molecular, cellular and tissue levels in proinflammatory remodeling of the arterial wall.
- The absence of MFG-E8 curtails Ang II induced adverse arterial remodeling via the decrease of proinflammation, VSMC proliferation, collagen deposition, and elastin fragmentation.

Significance

Ang II induced arterial proinflammatory remodeling is MFG-E8 genotype-dependent. Thus, targeting MFG-E8 signaling could be a novel molecular approach to prevent or treat Ang II associated adverse arterial remodeling.

Figure legends

Figure 1. Ang II infusion in both MFG-E8 KO and WT mice increases systolic blood pressure and circulating levels of Ang II and aortic MFG-E8 protein. **A.** Graph shows plasma Ang II concentrations ($p<0.001$ for overall treatment effect by repeated two-way ANOVA with the factors of treatment and genotype). Bar graph show mean ± SEM for KO and WT mice (n=5/group) with Ang II or saline infusion over time. **=$p<0.01$ and ***=$p<0.001$ by Bonferroni post-hoc testes following two-way ANOVA. **B.** Representative Western blots of aortic MFG-E8. **C**. Quantitative data of western blot of aortic MFG-E8, graph shows MFG-E8 protein abundance ($p<0.001$ for main Ang infusion effect, $p<0.001$ for main genotype effect, $p<0.001$ for treatment x genotype, by two-way ANOVA). Bar graph show mean ± SEM for KO and WT mice with Ang II or saline infusion (n=5/group). ***=$p<0.001$ by Bonferroni post-hoc tests following two-way ANOVA with the factors of treatment and genotype. **D.** Dynamic changes in mouse systolic blood pressure (SBP) measured by tail-cuffed method; plot shows mean ± SEM for KO and WT mice (n=5/group) with Ang II or saline infusion over time ($p<0.001$ for main treatment effect, $p<0.001$ for main genotype effect, $p<0.001$ for Ang II infusion x genotype, by repeated two-way ANOVA). ***=$p <0.001$ SBP in KO + Ang II vs KO + saline and WT + Ang II vs WT + saline group.

Figure 2. Ang II infusion enhances the activation of both circulating and aortic MMP-2 in WT mice. A. Representative zymograms of aortic gelatinases (**upper panel**). Quantitative graph (**lower panel**) shows activated MMP-2 protein abundance ($p<0.001$ for main treatment effect, $p<0.001$ for main genotype effect, $p<0.001$ for treatment x genotype, by two-way

ANOVA). Bar graph show mean ± SEM for KO and WT mice with Ang II or saline infusion (n=5/group). *p<0.05 and ***=p<0.001 by Bonferroni post-hoc testes following two-way ANOVA with the factors of treatment and genotype. **B.** Representative Western blots of aortic MMP-2, MT1MMP, and GAPDH (loading control). Graph shows quantitative data of (middle panel) aortic MMP-2 protein abundance (p<0.001 for main treatment effect, p<0.01 for main genotype effect, p<0.01 for treatment x genotype, by two-way ANOVA). Graph shows quantitative data of (right panel) aortic MT1MMP2 protein abundance (p<0.001 for main treatment effect, p<0.01 for main genotype effect, p<0.01 for treatment x genotype, by two-way ANOVA). Bar graph show mean ± SEM for KO and WT mice with Ang II or saline infusion (n=5/group). *=p<0.05, **=p<0.01, and ***=p<0.001 by Bonferroni post-hoc tests following two-way ANOVA with the factors of treatment and genotype.

Figure 3. Ang II infusion increases TGF-β1 activity and signaling within the aortic walls of WT mice. A. Representative Western blots of aortic TGF-β1, pSMAD2, and SMAD2. **B.** Graph shows quantitative data of (middle) aortic activated TGF-β1 protein abundance (p<0.001 for main treatment effect, p<0.001 for main genotype effect, p<0.001 for treatment x genotype, by two-way ANOVA). Graph shows quantitative data of (right) aortic pSMAD2/SMAD2 ration (p<0.001 for main treatment effect, p<0.001 for main genotype effect, p<0.01 for treatment x genotype, by two-way ANOVA). Bar graph show mean ± SEM for KO and WT mice with Ang II or saline infusion (n=5/group). *=p<0.05 and ***=p<0.001 by Bonferroni post-hoc testes following two-way ANOVA with the factors of treatment and genotype. **C**. Photomicrographs of immunostaining collagen type I (Collagen I) and morphometric analysis (right panel) shows relative collagen I immunostaining area (%) (p<0.001 for main treatment effect, p<0.001 for main genotype effect, p<0.001 for treatment x genotype, by two-way ANOVA). ***=p<0.001 by

Bonferroni post-hoc tests following two-way ANOVA with the factors of treatment and genotype. **D.** Representative Western blots of aortic Collagen I (low left panel). Graph shows quantitative data of (low right panel) aortic Collagen I ($p<0.01$ for main treatment effect, $p>0.05$ for main genotype effect, $p<0.0001$ for treatment x genotype, by two-way ANOVA). Bar graph show mean ± SEM for KO and WT mice with Ang II or saline infusion (n=4/group). ***=$p<0.001$ by Bonferroni post-hoc tests following two-way ANOVA with the factors of treatment and genotype. L=lumen; M=media. Scale bar= 100μm.

Figure 4. Ang II infusion enhances aortic transcription factor NF-κB activation and its downstream molecules in WT mice. A. Representative Western blots of aortic NF-κB p65, MCP-1, TNF-α1, and GAPDH (left panels). Graph (left panel) shows quantitative data of NF-κB p65 protein abundance ($p<0.001$ for main treatment effect, $p<0.001$ for main genotype effect, $p<0.001$ for treatment x genotype, by two-way ANOVA). Bar graph show mean ± SEM for KO and WT mice with Ang II or saline infusion (n=5/group). *=$p<0.05$ and ***=$p<0.001$ by Bonferroni post-hoc tests following two-way ANOVA with the factors of treatment and genotype. Graph (middle panel) shows quantitative data of MCP-1 protein abundance ($p<0.01$ for main treatment effect, $p<0.05$ for main genotype effect, $p<0.001$ for treatment x genotype, by two-way ANOVA). Bar graph show mean ± SEM for KO and WT mice with Ang II or saline infusion (n=5/group). ***=$p<0.001$ by Bonferroni post-hoc tests following two-way ANOVA with the factors of treatment and genotype. Graph (right panel) shows quantitative data of TNF-α1 protein abundance ($p<0.001$ for main treatment effect, $p>0.05$ for main genotype effect, $p<0.05$ for treatment x genotype, by two-way ANOVA). Bar graph show mean ± SEM for KO and WT mice with Ang II or saline infusion (n=5/group). ***=$p<0.001$ by Bonferroni post-hoc tests following two-way ANOVA with the factors of treatment and genotype. **B**.

Photomicrographs of immunostaining of TNF-α. Graph shows quantitative data of (right panel) aortic TNF-α1immunostaing area (%) ($p<0.01$ for main treatment effect, $p<0.05$ for main genotype effect, $p<0.01$ for treatment x genotype, by two-way ANOVA). Bar graph show mean ± SEM for KO and WT mice with Ang II or saline infusion (n=5/group). *=$p<0.05$ and ***=$p<0.001$ by Bonferroni post-hoc tests following two-way ANOVA with the factors of treatment and genotype. C**.** Photomicrographs of Immunostaining ICAM1 and morphometric analysis (right panel) shows relative ICAM1 immunostaining area (%) ($p<0.001$ for main treatment effect, $p<0.001$ for main genotype effect, $p<0.001$ for treatment x genotype, by two-way ANOVA). ***=$p<0.001$ by Bonferroni post-hoc tests following two-way ANOVA with the factors of treatment and genotype. **D.** Photomicrographs of immunostaining VCAM1 and graph (right panel) shows relative VCAM1 staining area (%) ($p<0.001$ for main treatment effect, $p<0.001$ for main genotype effect, $p<0.001$ for treatment x genotype, by two-way ANOVA). ***=$p<0.001$ by Bonferroni post-hoc tests following two-way ANOVA with the factors of treatment and genotype. L=lumen; M=media. Scale bar= 100µm.

Figure 5. Ang II infusion increases aortic remodeling in WT mice. A. Photomicrographs of hematoxylin-eosin (HE) staining of aortic walls. Graph shows (far right panel) the ratio of aortic intimal medial area to luminal area ($p<0.001$ for main treatment effect, $p<0.001$ for main genotype effect, $p<0.001$ for treatment x genotype, by two-way ANOVA). **B.** Photomicrographs of Elastin Verhoeff's-Van Gieson (EVG staining) of aortic walls. Graph shows (far right panel) elastin breaks ($p<0.05$ for main treatment effect, $p<0.001$ for main genotype effect, $p<0.01$ for treatment x genotype, by two-way ANOVA). **C.** Photomicrograph of Masson's trichrome staining of aortic walls. Graph shows extracellular matrix (ECM) (blue color) ($p>0.05$ for main treatment effect, $p<0.01$ for main genotype effect, $p<0.01$ for treatment x genotype, by two-way

ANOVA). **D.** Photomicrographs of proliferation cellular nuclear antigen (PCNA) immunostaining of aortic walls. Graph shows (far right panel) relative PCNA stained area ($p>0.05$ for main treatment effect, $p<0.01$ for main genotype effect, $p<0.01$ for treatment x genotype, by two-way ANOVA). Bar graph show mean ± SEM for KO and WT mice with Ang II or saline infusion (n=5/group). *=$p<0.05$, **=$p<0.01$ and ***=$p<0.001$ by Bonferroni post-hoc tests. L=lumen; M=media. Scale bar= 100µm.

Figure 6. Interactions of MFG-E8 and Ang II during proinflammatory arterial remodeling.

Table 1. Information on primary antibodies.

Antibody	Company	Cat#	Titer for WB	Titer for IHC
MFG-E8	R&D Systems	AF2805	1:1000	
MMP-2	R&D Systems	AF1488	1:500	
MT1-MMP	Thermo Fisher Scientific	PA5-16514	1:500	
Smad2	Santa Cruz Biotechnology	5339	1:1000	
p-Smad2	Santa Cruz Biotechnology	3108	1:500	
NF-κB-p65	Santa Cruz Biotechnology	sc-8008	1:500	
TGF-β1	Santa Cruz Biotechnology	sc-146	1:200	
MCP1	R&D Systems	AF479	1:200	
TNF-α	Abcam	ab9739	1:1000	1:100
ICAM1	Santa Cruz Biotechnology	Sc-8439		1:50
VCAM1	Santa Cruz Biotechnology	Sc-13160		1:50
GAPDH	Cell Signaling technology	5014	1:1000	
PCNA	Santa Cruz	sc-9857		1:50
Collagen I	Santa Cruz	sc-59772		1:50

WB=western blotting; IHC=immunohistochemistry

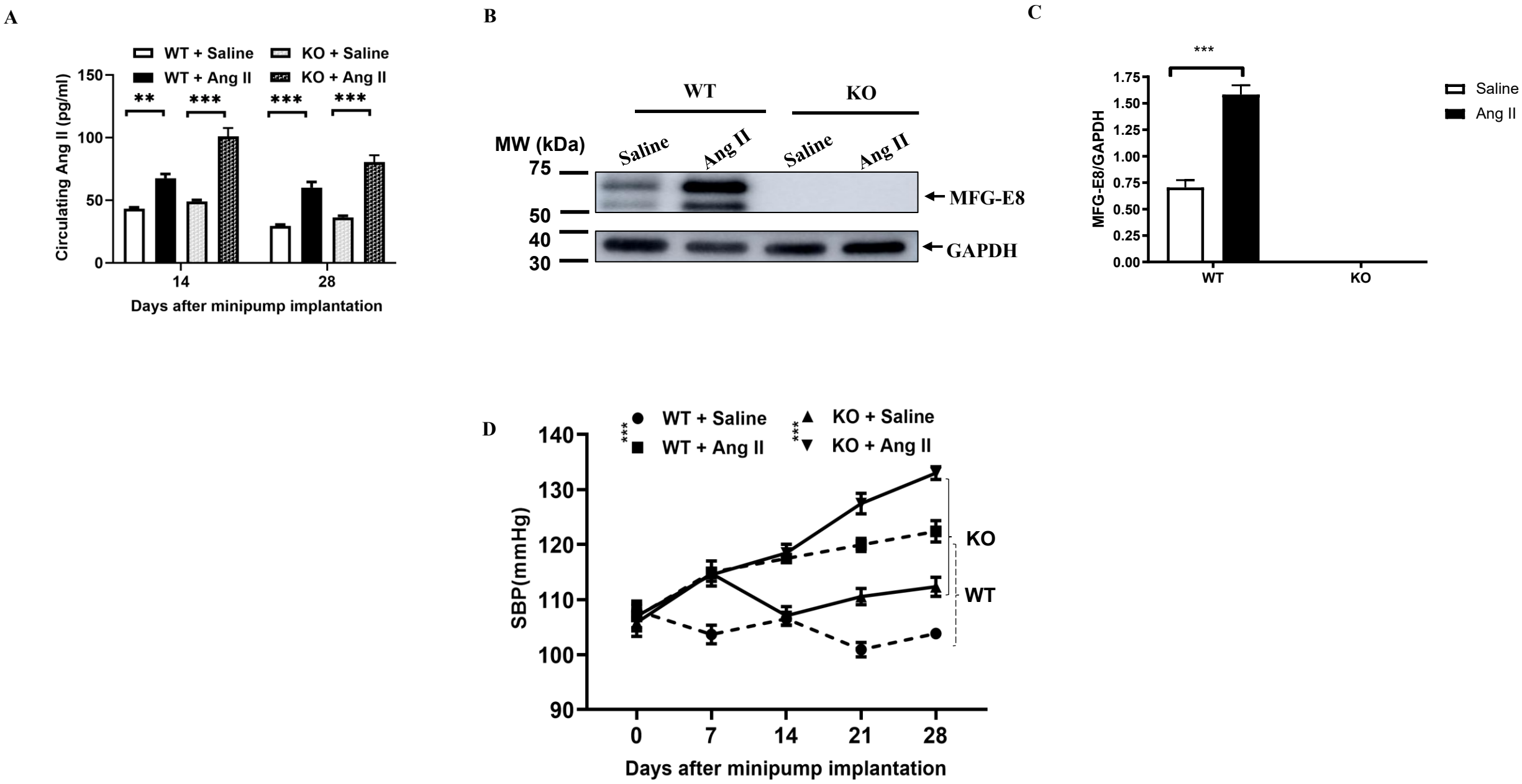
A
WT + Saline
WT + Ang II
KO + Saline
KO + Ang II
Circulating Ang II (pg/ml)
150
100
50
0
**
***
***
***
14
28
Days after minipump implantation
B
WT
KO
MW (kDa)
Saline
Ang II
Saline
Ang II
75
50
40
30
MFG-E8
GAPDH
C
***
MFG-E8/GAPDH
1.75
1.50
1.25
1.00
0.75
0.50
0.25
0.00
WT
KO
Saline
Ang II
D
WT + Saline
WT + Ang II
KO + Saline
KO + Ang II
***
***
SBP(mmHg)
140
130
120
110
100
90
0
7
14
21
28
Days after minipump implantation
KO
WT

Figure 1

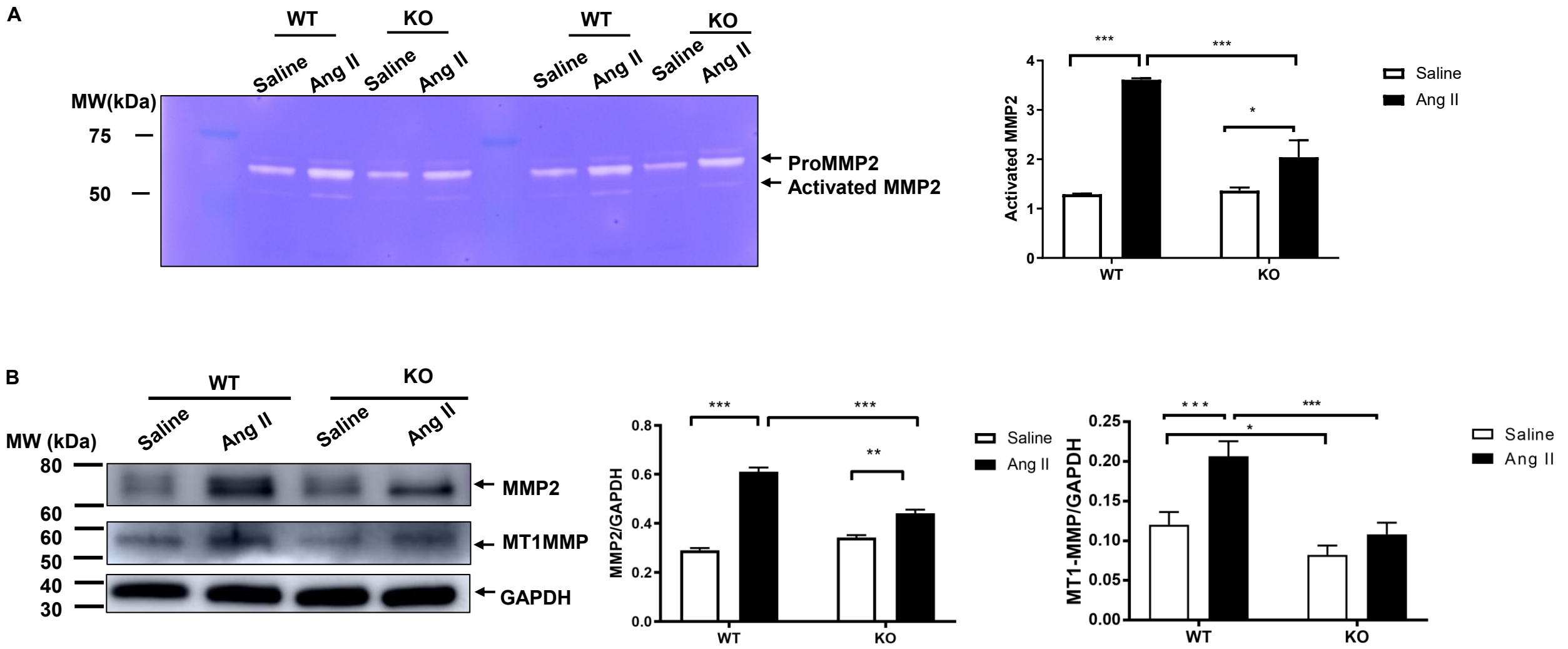
A
WT
KO
WT
KO
Saline
Ang II
Saline
Ang II
Saline
Ang II
Saline
Ang II
MW(kDa)
75
50
ProMMP2
Activated MMP2
Activated MMP2
Saline
Ang II
WT
KO
B
WT
KO
Saline
Ang II
Saline
Ang II
MW (kDa)
80
60
60
50
40
30
MMP2
MT1MMP
GAPDH
MMP2/GAPDH
Saline
Ang II
WT
KO
MT1-MMP/GAPDH
Saline
Ang II
WT
KO

Figure 2

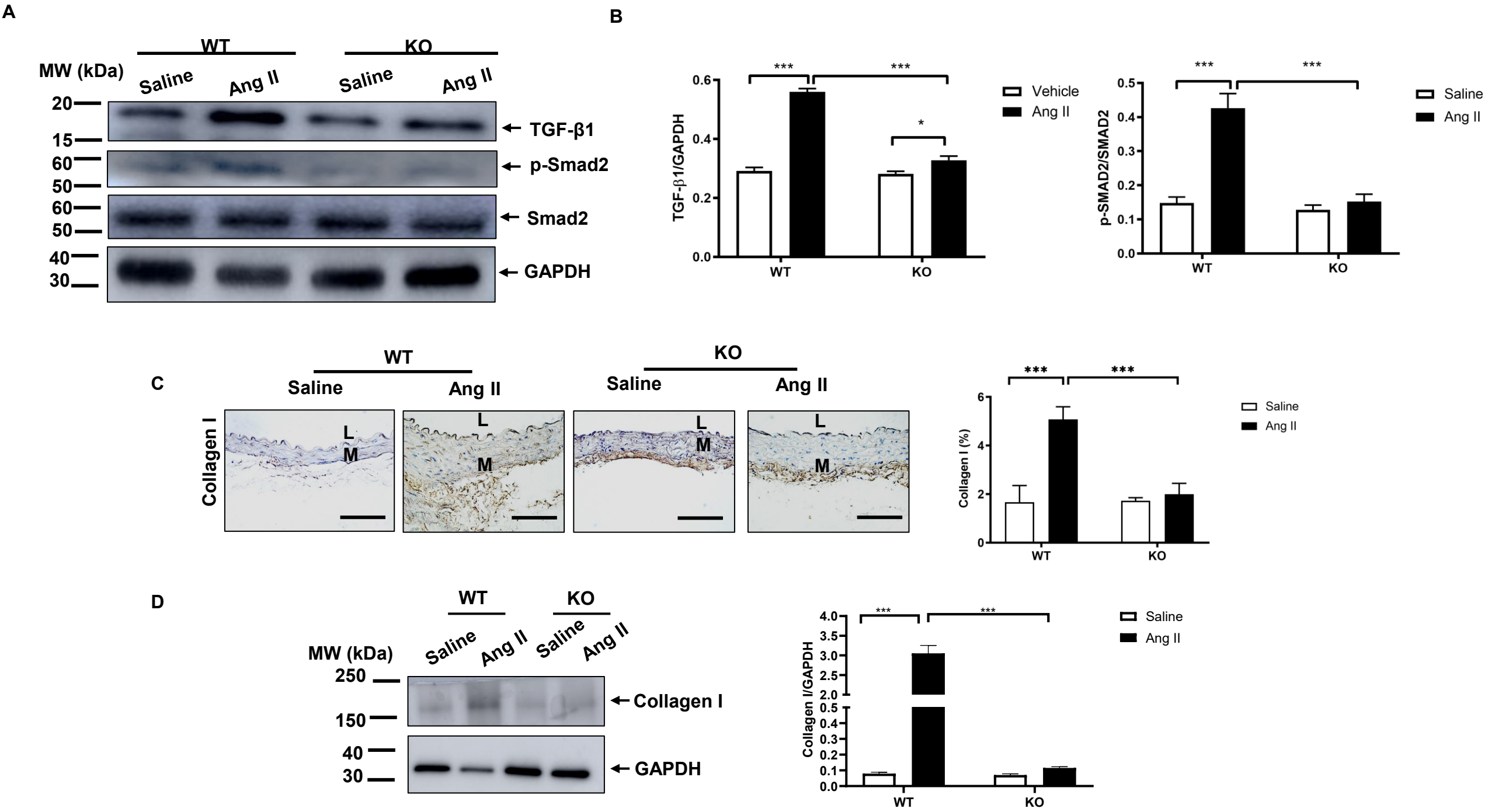
A
WT
KO
MW (kDa)
Saline
Ang II
Saline
Ang II
20
15
60
50
60
50
40
30
TGF-β1
p-Smad2
Smad2
GAPDH
B
TGF-β1/GAPDH
Vehicle
Ang II
WT
KO
p-SMAD2/SMAD2
Saline
Ang II
C
Collagen I
L
M
Collagen I (%)
D
MW (kDa)
250
150
40
30
Collagen I
GAPDH
Collagen I/GAPDH

Figure 3

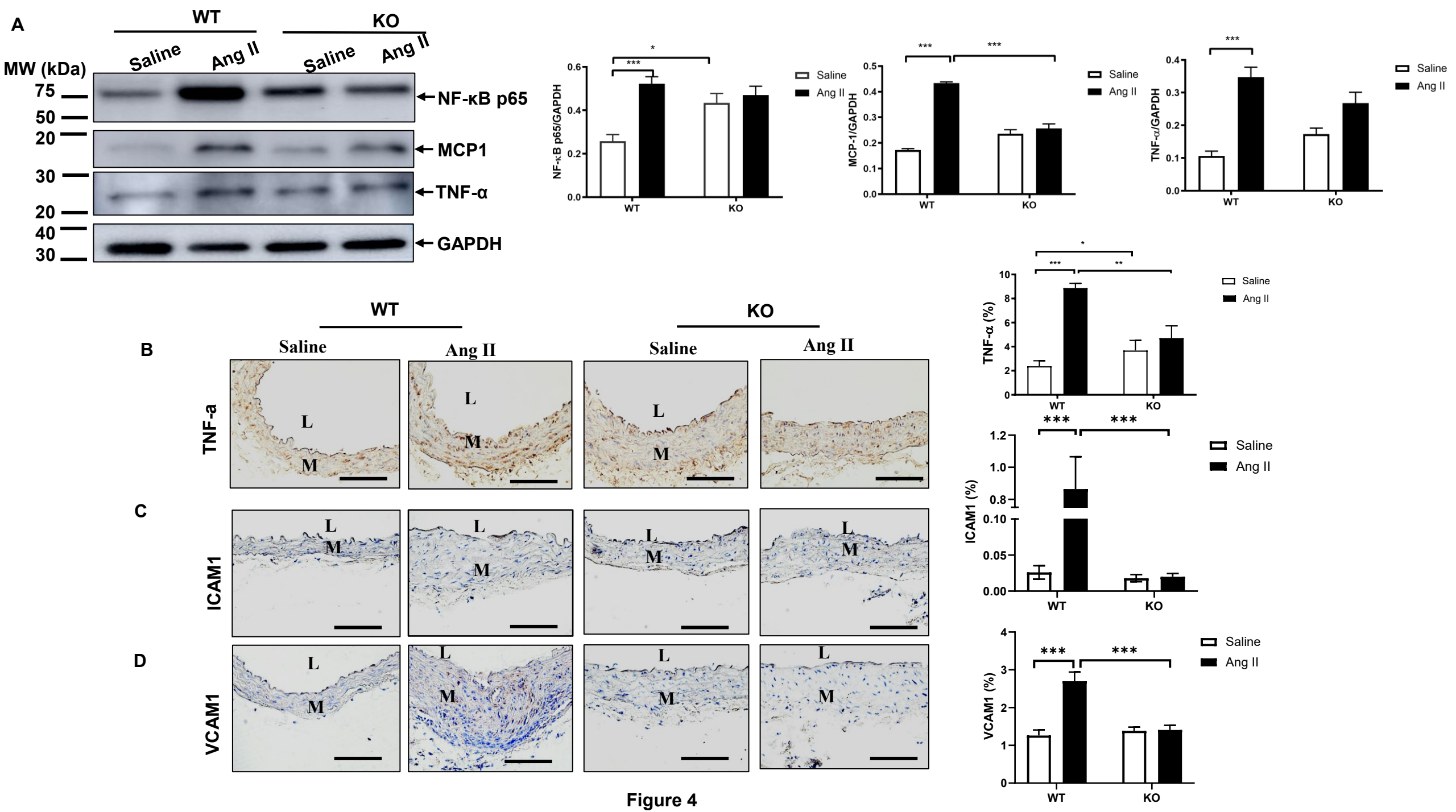
A
WT
KO
Saline
Ang II
Saline
Ang II
MW (kDa)
75
50
20
30
20
40
30
NF-κB p65
MCP1
TNF-α
GAPDH
NF-κB p65/GAPDH
MCP-1/GAPDH
TNF-α/GAPDH
Saline
Ang II
WT
KO
B
C
D
TNF-a
ICAM1
VCAM1
L
M
TNF-α (%)
ICAM1 (%)
VCAM1 (%)

Figure 4

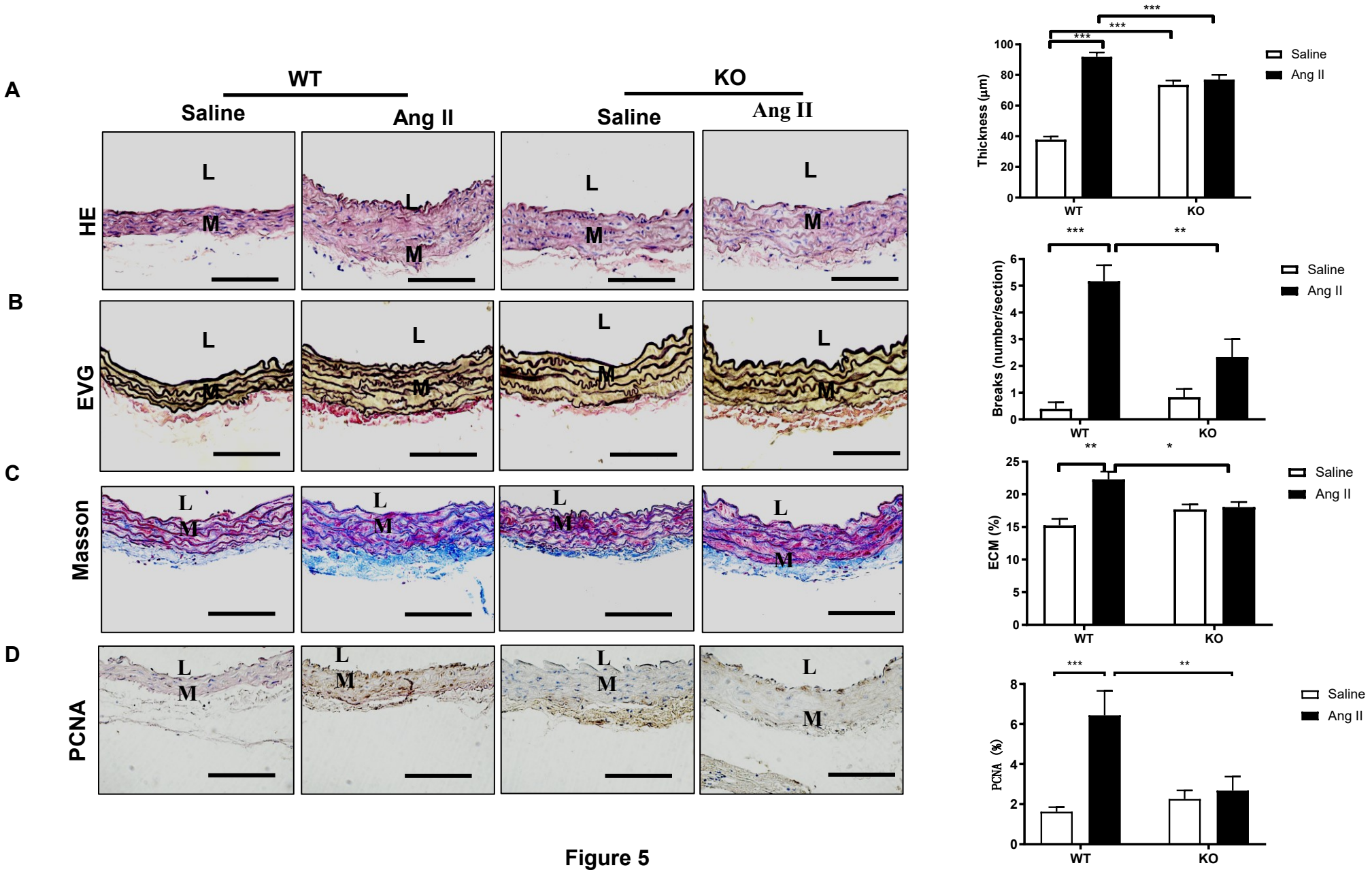
A
WT
KO
Saline
Ang II
Saline
Ang II
HE
B
EVG
C
Masson
D
PCNA
L
M
Thickness (μm)
Breaks (number/section)
ECM (%)
PCNA (%)
WT
KO
Saline
Ang II
***
**
*

Figure 5

The Role of MFG-E8 in Aortic Proinflammatory Remodeling

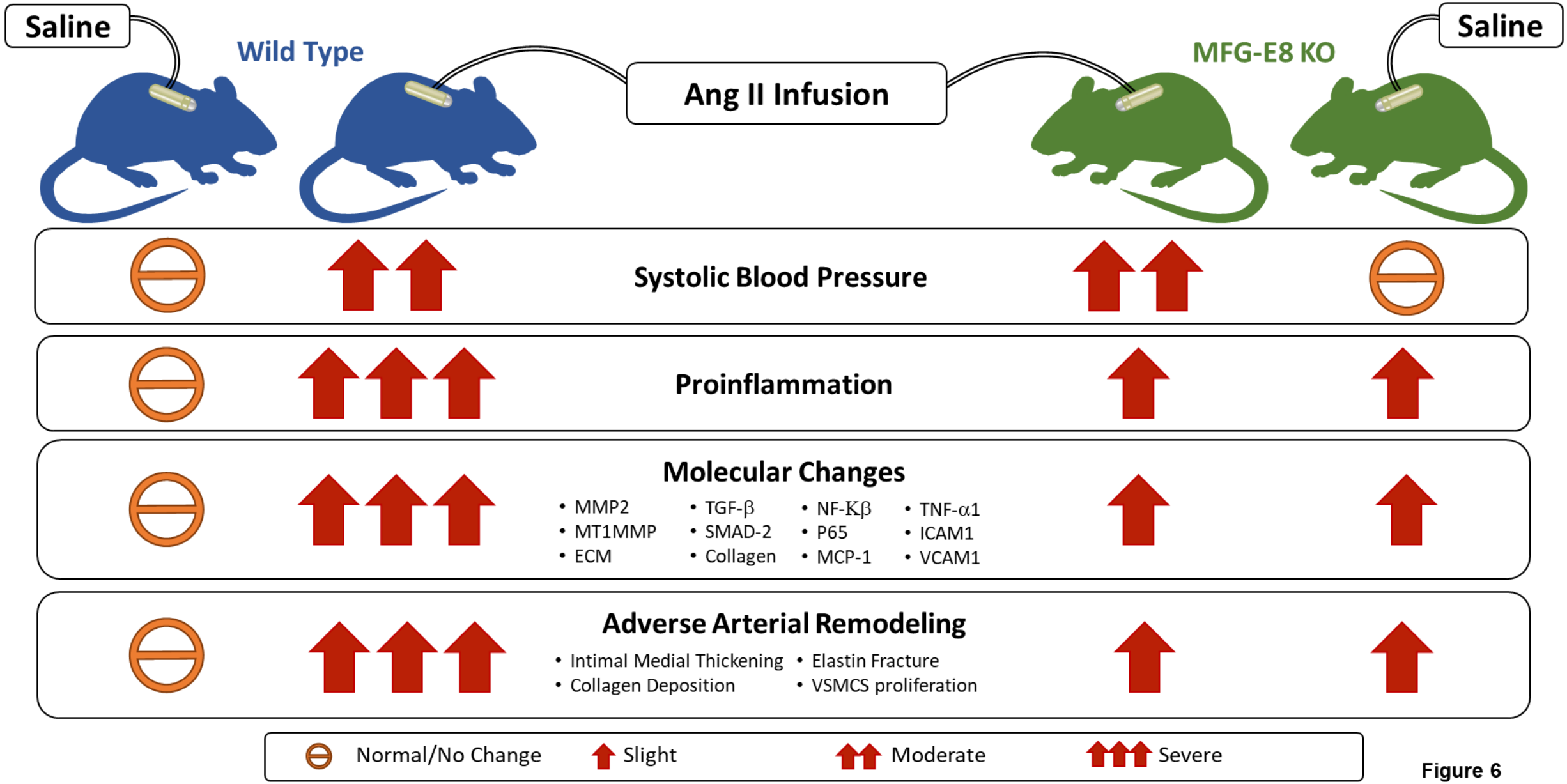

Figure 6